Please refer to this article using:

Frankl, A., Poesen, J., Mitiku Haile, Deckers, J., Nyssen, J., 2013. Quantifying long-term changes in gully networks and volumes in dryland environments: the case of Northern Ethiopia, Geomorphology, 201, 254-263. 10.1016/j.geomorph.2013.06.025

- Check the website of Geomorphology for the final version of this publication

Quantifying long-term changes in gully networks and volumes in dryland environments: the case of Northern Ethiopia

Amaury Frankl [a,*], Jean Poesen [b], Mitiku Haile [c], Jozef Deckers [b], Jan Nyssen [a]

[a] Department of Geography, Ghent University, Krijgslaan 281 (S8), B-9000 Ghent, Belgium.

[b] Department of Earth and Environmental Sciences, KU Leuven, B-3001 Heverlee, Belgium.

[c] Department of Land Resources Management and Environmental Protection, Mekelle University, Mekelle, Ethiopia.

* Corresponding author: Tel.: +32 92644701; fax: +32 92644985; e-mail address: amaury.frankl@ugent.be (A. Frankl)

Abstract

Understanding historical and present gully development is essential when addressing the causes and consequences of land degradation, especially in vulnerable dryland environments. For Northern Ethiopia, several studies exist on the severity of gully erosion, yet few have quantified gully development. In this study, gully network and volume development were quantified over the period 1963-2010 for an area of 123 km², representing the regional variability in

environmental characteristics. Gully networks were mapped from small-scale aerial photographs and high-resolution satellite images. For the latter, visualizing Google Earth images in 3D proved to be very suitable to investigate gully erosion. From the changes in networks and volumes over the period 1963-2010, the occurrence of one cut-and-fill cycle is apparent. From a largely low-dynamic gully system in the 1960s, network expansion and increased erosion rates in the 1980s and 1990s caused the drainage density and volume to peak in 1994. The average gully density (D_{total}) was then 2.52 km km^{-2} and the area-specific gully volume (V_a) 60 10³ m³ km^{-2}. This coincides with soil losses by gully erosion (SLg) of 17.6 t ha^{-1} y^{-1} over the period 1963-1994. By 2010, improved land management and the region-wide implementation of soil and water conservation measures caused 25% of the gully network to stabilize, resulting in a net infilling of the gully channels over the period 1994-2010. The study validates previous findings that land degradation by gullying was indeed severe in Northern Ethiopia in the second half of the 20th century, but also shows that when proper land management is applied, a gully can be transformed into a linear oasis, which increases the resistance of gullies to further erosion.

Keywords: Aerial photographs; Dryland; Ethiopia; Google Earth; Gully; Volume

1. Introduction

Drylands are areas where evapotranspiration exceeds precipitation during part of, or during, the whole year (Kassas, 1995). They cover 40% of the Earth's surface and house about 2.1 billion people in nearly 100 countries, including Ethiopia (UNEP-DDD, 2012). In terms of aridity, drylands are defined as regions where the ratio between long-term annual precipitation and potential evapotranspiration is between 0.05 and 0.65, and include hyper-arid, arid, semi-arid and

48 dry sub-humid zones (Thornthwaite, 1948; UNEP, 1994). For these zones, water availability and
49 biomass production are restricted and mostly confined to a short rainy season. As a result, the
50 carrying capacity of the ecosystems is rapidly exceeded by the human exploitation of natural
51 resources, especially in poor countries with fast demographic expansion and deficient
52 exploitation techniques (Kassas, 1995). Furthermore, the resilience of drylands is often reduced
53 by the occurrence of recurring droughts and severe desertification, which threatens sustainable
54 development in these fragile environments.
55 Gully erosion is acknowledged as a key erosion process whereby land degradation in dryland
56 environments occurs. In a review, Poesen et al. (2002) conclude that gully erosion contributes to
57 50% to 80% of the overall sediment production in drylands. Sediment yields are locally very
58 variable, but may be as high as 3.4 t ha^{-1} y^{-1} in Kenya, 32 t ha^{-1} y^{-1} in Niger, 16.1 t ha^{-1} y^{-1} in
59 Portugal, 64.9 t ha^{-1} y^{-1} in Spain and 36.8 t ha^{-1} y^{-1} in the USA (Poesen et al., 2003).
60 Understanding historical and present-day gully erosion is therefore essential when addressing the
61 consequences of future land-use and climate change scenarios (Poesen et al., 2003; Valentin et
62 al., 2005). For instance, land managers need to foresee the effects of land-use changes,
63 infrastructure construction or urbanization on gully development. Without such projections,
64 future developments may be unsustainable and yield much higher costs than originally budgeted.
65 In addition, soil losses may strongly increase, jeopardising in-situ and downstream agricultural
66 production (Poesen et al., 2003). Furthermore, the rapid expansion of gullies is related to shifts in
67 the hydrological regime of landscapes (Knighton, 1998), by which runoff and soil water rapidly
68 converge to gullies (Muhindo Sahani, 2011). This often results in flash floods of polluted water
69 which threaten human health.

Relatively few studies investigate the importance of gully erosion on land degradation, especially when considering sub-Saharan Africa (e.g., Stocking, 1980; Moeyersons, 1989, 1991; Boardman et al., 2003; Katsurada, 2007; Marzolff and Ries, 2007; Leblanc et al., 2008; Ndona and Truong, 2011). From the studies that report on severe historical and present gully erosion in Ethiopia (e.g., Virgo and Munro, 1978; Nyssen et al., 2002; Billi and Dramis, 2003; Reubens et al., 2009; Frankl et al., 2011), few quantified gully erosion networks or volumes over large areas. Nyssen et al. (2006) investigated the development of four gully systems in Northern Ethiopia by developing a field method which is based on how local people remember the historical extent of gullies. Although this approach yields accurate results, it is rather difficult to apply over large areas. That is why, in Southern Ethiopia, Moges and Holden (2008) limited their analysis on the importance of historical gully erosion to eight gullies. A small gully network in Eastern Ethiopia was studied by Daba et al. (2003), using a time-series of Digital Elevation Models (DEMs) derived from small-scale aerial photographs. Analyzing the development of gully headcuts and cross-sections at regional scale was done by Frankl et al. (2011, 2012).

The objective of this paper is to quantify changes in gully networks and volumes since 1963 in Northern Ethiopia from remote sensing data. The presented methods are widely applicable, as coverage by aerial photographs and satellite images are common over long periods in many areas, including dryland environments. The results are representative for the broader region and reflect the importance of gully erosion in drylands. Moreover, the linkages with the controlling factors of gully erosion are discussed.

2. Materials and Methods

2.1. Study area

93 Eight catchments, representative for the regional variability in environmental characteristics,
94 were selected to study gully development in Northern Ethiopia: Ablo (15.2 km²), May Mekdan
95 (44.7 km²), May Ba'ati (4 km²), May Tsimble (8.1 km²), Atsela (4.9 km²), Ayba (37 km²),
96 Seytan (8.2 km²) and Lake Ashenge (1.1 km²) (Figure 1). The study areas have elevations that
97 range between 2100 and 3900 m a.s.l., and consist of deeply incised valleys which developed
98 with the uplift of Ethiopian Highlands at the western margin of the Rift Valley (Williams and
99 Williams, 1980). The Ablo catchment exposes sandstone; May Mekdan and May Tsimble shale
100 with limestone cliffs and occasionally dolerite at the summits; Atsela, Ayba, Seytan and Lake
101 Ashenge expose volcanics (flood basalt, rhyolites and consolidated volcanic ash) and May Ba'ati
102 exposes volcanics at higher elevations, while sandstone, limestone and shale occur at lower
103 elevations.
104

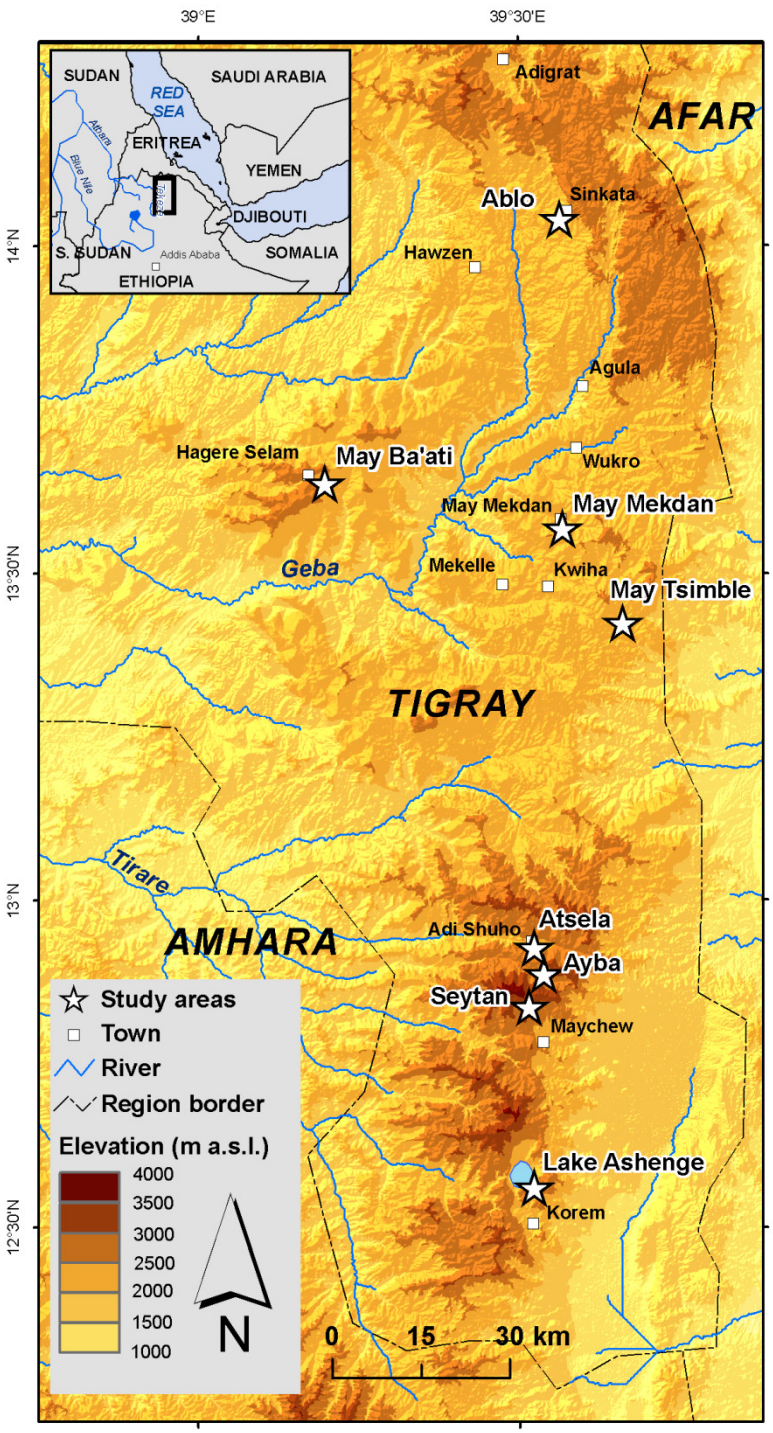

105

106 **Figure 1**: Location of the study areas in the Northern Ethiopian Highlands. Oro-hydrography

107 based on SRTM data (http://srtm.csi.cgiar.org).

108

109 Rainfall is mostly restricted to a short rainy season from July until early September. Average
110 annual rain increases from north to south, ranging between 500 and 900 mm y^{-1}, and usually
111 falls as intense showers that seldom last longer than ten minutes (Nyssen et al., 2005). Rain is
112 however highly unreliable and droughts frequently occur.
113 Due to active geomorphologic processes, most soils are young (HTS, 1976; Nyssen et al.,
114 2008a). Leptosols are found in high landscape positions while Regosols or Cambisols occur on
115 steep slopes. In footslope positions, more developed fine-textured soils occur, with Vertisols on
116 basalt (colluvium) and Calcisols on limestone. Under remnant forests, Phaeozems occur
117 (Descheemaeker et al., 2006).
118 Land degradation is severe in Northern Ethiopia (Virgo and Munro, 1978; Nyssen et al., 2004).
119 Gullies affect nearly all slopes and frequently exceed 2 m in depth and 5 m in top width. Their
120 occurrence is related to the vulnerable environment, which exposes steep slopes, where rainfall
121 intensities are high and where deforestation and overgrazing depleted the landscape of most
122 vegetation. However, with the introduction of soil and water conservation measures since the
123 1970s – including slope terracing, the establishment of exclosures, and the construction of check
124 dams in gullies – the landscape is greening and reports on land rehabilitation are becoming more
125 frequent (e.g., McCann, 1997; Crummey, 1998; Nyssen et al., 2009; Munro et al, 2008).
126
127 2.2. Creating time-series of aerial photographs and satellite images
128 A database of satellite images and digitized stereographic aerial photographs was created for all
129 eight study areas. Aerial photographs of 1963, 1965, 1986 and 1994 having scales ranging
130 between 1:35,000 and 1:60,000 (ground resolutions of 1-2 m) were collected from the Ethiopian
131 Mapping Authority. They were scanned at a resolution of 1200 dpi with a desktop scanner.

IKONOS-2 satellite images (resolution of 1 m) of 2006 were available from the VLIR MU-IUC program for the study areas of Ablo and May Ba'ati. For all other study areas, images were consulted on Google Earth. This platform offers high resolution GeoEye - 1 (resolution of 0.50 m) images of 2005, Digital Globe (resolution of 0.60 m) images of 2006, and Cnes SPOT (resolution 2.5 m) images of 2011, and allows 3D visualization of the images.

Next, the aerial photographs and satellite images were geometrically rectified into the UTM-WGS1984 coordinate system. Considering the satellite images, a good rectification was already provided by reading the IKONOS-2 images into ArcGIS 9.2 together with the period rational polynomial coefficient (RPC) data. In order to increase the accuracy for the areas of interest, Ground Control Points (GCPs) were used to perform a second order polynomial transformation on the images. Considering the aerial photographs, the geometric rectification was done from a photogrammetric restitution (Miller, 2004) or, when this yielded poor results, from a co-registration (Hughes et al. 2006; James et al., 2012). Photogrammetric restitutions were done with Supersoft Inc VirtuoZo 2.2 and were based on a DEM devised for the same area. Producing DEMs from the aerial photographs required inner and exterior orientation. The relative orientation was based on >300 tie points per stereo pair, and the exterior orientation on seven to fifteen GCPs. When the number of GCPs suitable for the DEM production was too low for a specific area and period, the photogrammetric restitution proved to be unsuccessful. This was especially the case when considering the oldest aerial photographs that display a landscape that has undergone important changes. Within decades of fast population growth, rural settlements, infrastructure and land management structures may have changed considerably. Moreover, the low level of technological development implies that few human-built structures were stable. For instance, the position of footpaths may change over time, trees may be cut and traditional houses

and fences rebuilt. Therefore, the geometric rectification of some aerial photographs was done by co-registration. Second or third order polynomial transformations (with ArcGIS 9.2) were performed, using points that were derived from the most recent orthophotographs or Google Earth images. The advantage of such an image-to-image registration is that a large number of corresponding points can be identified on both layers, assuring a density of 2 to 9 points per km². As shown by Hughes et al. (2006) and James et al. (2012), such an approach can yield reasonable results when considering small areas and using enough control points that are located close to the features of interest.

Once all photographs and images were geometrically rectified, they were organized as layers in a Geographic Information System (GIS) environment. Switching the layers on or off allows easy and rapid observations of gully network changes in the study areas. As could be visually observed, some orthophotographs produced from DEMs showed relatively large lateral displacements when compared to each other. This was solved by performing a co-registration of these layers to the most recent image. As a result, observed changes in the gully networks that were the result of mismatches between the different layers were kept minimal.

Assessing the horizontal positional accuracy was done for each layer by calculating the distance between an independent set of ten ground control points measured by GPS in the field, and their location on the different layers. This approach quantifies the horizontal error that is not influenced by the type of data used, or the way in which they were geometrically rectified. Consequently, the average horizontal positional error (± standard deviation) for the different layers could be compared with each other. Table 1 indicates that all the layers have a similar horizontal positional accuracy, which is not related to the type of rectification process. For all periods and catchments the average horizontal positional accuracy was 8.4±3.3 m. In some cases,

178 observations from one layer were transferred to another. This was done for the 1963 situation of
179 the Seytan catchment, for which only 47% of the catchment could be observed, and for the
180 situations of Atsela 1965 and 1986, and Lake Ashenge 1986 and 1994, which were largely
181 adapted from Frankl et al. (2011).
182

Table 1. Horizontal positional accuracy of the produced dataset. The average locational error ± standard deviation is based on 10 independend test points that were measured in the field by Trimble® GEO XH 2005 series GPS with submeter accuracy.

		Year					
		1963	1965	1974	1986	1994	2005-2011
Catchment	Ablo					12.6±7.3 [c]	6.7±3.8 [b]
	May Mekdan		8.1±3.2 [a]			5.5±3.4 [a]	
	May Ba'ati	9.6±4.8 [a]		7.1±4.4 [c]		7.0±4.4 [a]	5.6±2.7 [b]
	May Tsimble					16.4±10.0 [c]	12.6±8.2 [b]
	Astela [d]		TRANS 1994		TRANS 1994	9.3±5.6 [a]	5.1±1.8 [b]
	Ayba		7.2±3.2 [c,e]		10.4±6.1 [c]	12.9±6.6 [a,c]	5.1±1.8 [b]
	Seytan	TRANS 1994 [f]			10.6±5.6 [c]		5.1±1.8 [b]
	Lake Ashenge [d]		6.7±2.5 [a]		TRANS 2006	TRANS 2006	5.1±1.8 [b]

(a) Orthophotograph; (b) Satellite image; (c) Georectified aerial photograph; (d) Data largly adapted from Frankl et al. (2011); (e) 91% of the catchment could be observed; (f) 47% of the catchment could be observed.
TRANS 1994: transfered to the 1994 situation

183

184 The accuracy of the gully network maps depends on (i) the horizontal positional accuracy of the
185 data-layers, (ii) the ability to detect the gully networks on the aerial photographs and satellite
186 images, which depends on the spatial resolution of the layers and the ability to distinguish gullies
187 from adjacent land covers, and (iii) errors in the vectorisation process within the GIS software.
188 As shown by Frankl et al. (2013a), who mapped gully networks both from Google Earth images
189 and from ground measurements (May Ba'ati 2008-2010 in this study, Table 2), these errors result
190 in both under- and overestimations of gully length, which resulted in an average error of 7.5% on
191 the drainage density as computed from the imagery alone. The most important errors are related

192 to difficulties in correctly identifying gullies in low-contrast areas, which is very similar for all
193 aerial photographs and images used in this study. Therefore, we assumed an error of 7.5%
194 (Frankl et al., 2013a) on the network density calculation in this study (see Section 2.2.).
195
196 2.2. Quantifying changes in gully networks and volumes
197 Gully networks observed on the time-series of aerial photographs and satellite images were
198 mapped on-screen using ArcGIS 9.2 or Google Earth, and were updated with more recent
199 modifications as observed in the field (period 2008-2010). For each period, a distinction was
200 made between low-active and high-active gullies (Figure 2) using criteria similar as those used
201 by Oostwoud Wijdenes et al. (2000). Low-active gullies typically have a narrow active channel,
202 smooth cross-sectional profiles, and walls overgrown by vegetation; and mobile bed material is
203 absent or restricted to small grain sizes. For the most recent period, stabilization of low-active
204 channels was typically enforced by check dams. High-active gullies are characterized by an
205 active channel width equal to the total width of the gully bottom. Therefore, the channel has a
206 rectangular cross-sectional shape with steep, well-delineated walls subject to mass failure.
207 Vegetation is not present on the channel floor and on the lower section of the walls. Mobile bed
208 material is present, especially in the lower sections of the gullies where sediment deposition
209 becomes more important. Furthermore, recent peak flow discharges in the gully can be assessed
210 by the size of the entrained bed particles and by flood marks in the gully channel.
211 For the most recent situation, field observations allowed to classify the gully networks into
212 low- and high-active segments. This was accompanied by observing the high-resolution
213 satellite images available in Google Earth. For previous periods, for which aerial
214 photographs were used to map gully networks, the distinction between low- and high-active

gullies was made visually by observing the gully segments in stereographic view. The steep and well delineated walls make the high-active gullies very distinctive. Their detection is often accentuated by shadows cast in the gullies and by the absence of vegetation. Making the distinction between low- and high-active gullies from aerial photographs requires expertise in gully erosion and good practice with using aerial photographs, and therefore, remains to a certain extent subjective. Validating the classification of historical gully networks into low- or high-active segments was therefore done by using a large dataset of historical terrestrial photographs (Frankl et al., 2011) that show the gully networks in the same periods as that of the aerial photographs, and from which gully activity could be assessed easily. Before analyzing changes in gully network development, networks mapped in Google Earth were integrated in ArcGIS 9.2 by the method of Frankl et al. (2013a). Subsequently, the gully network density could be calculated and analyzed for the different study areas and periods.

A preliminary study on the controls of the drainage density was made by analyzing the effect of catchment area (A, in km²), lithology and average catchment slope gradient (S_c, in m m^{-1}) of 21 subcatchments smaller than 10 km². A was mapped from contour lines derived from DEMs or from topographical maps and was verified in the field, S_c was obtained from SRTM data (90 m resolution, available on http://srtm.csi.cgiar.org), using ArcGIS 9.2 (Spatial Analyst). The effects of A and S_c were analyzed with a linear regression ($\alpha = 0.05$) and the effects of lithology with Analysis of Variance (one-way ANOVA, $\alpha = 0.05$).

Quantifying gully volumes was done in the field for the most recent situation of 2008-2010 (Frankl et al., 2013b). By considering 33 mutually exclusive catchments, totaling 5 380 ha and 152 km of gully length, gully volume (V) – length (L) relationships were established, taking the regional environmental variability and gully characteristics into account. As the lithology and the

presence of check dams or low-active channels proved to be the most important controls of gully cross-sectional shape and size, $V - L$ relationships were established for the different lithologies and percentages of the gully network having check dams and/or being low active (Frankl et al., 2013b). These equations (having r^2 values ranging between 0.81 and 0.94) could then be applied to historical gully networks to calculate their volumes taking into account the gully cross-sectional variability.

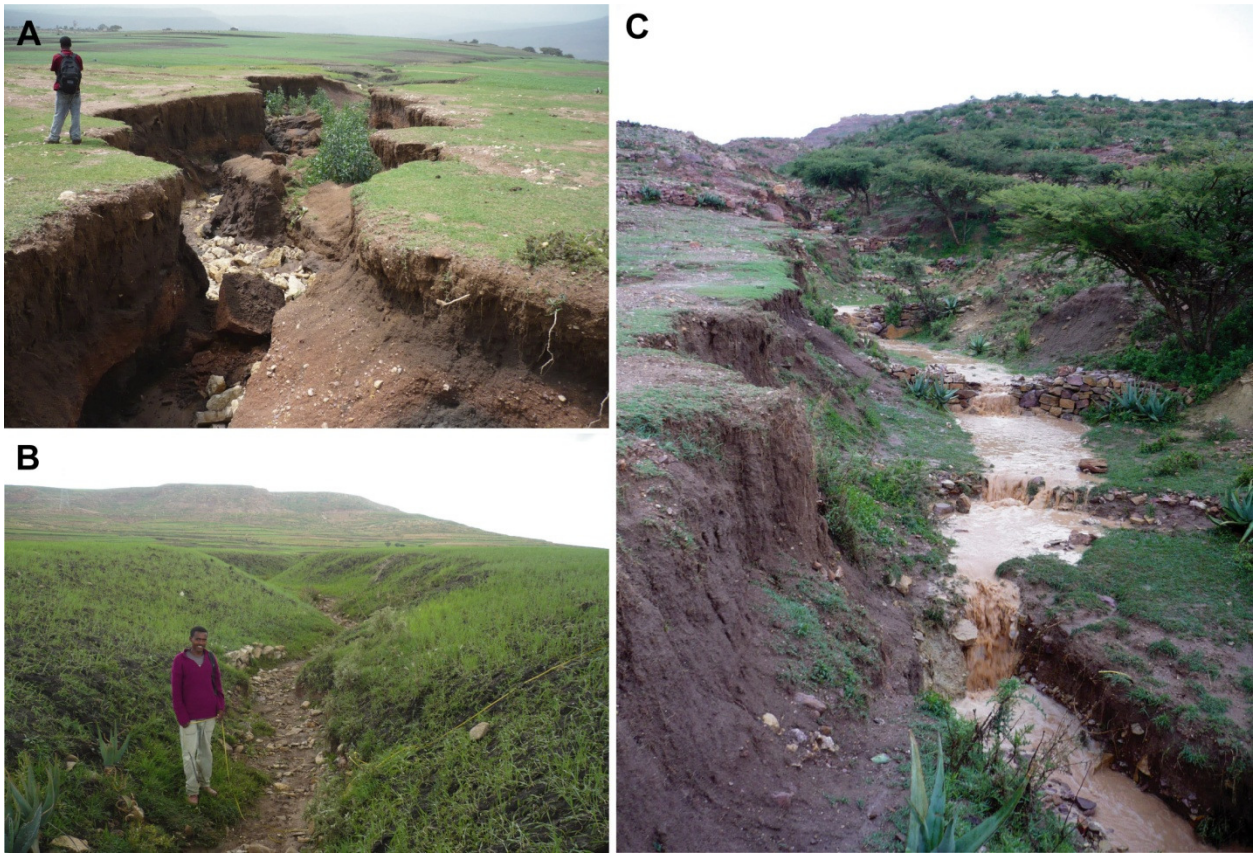

Figure 2: Examples of high- and low-active gully segments. **A**: High-active gully section, **B**: Low-active section without check dams and **C**: Low-active section with check dams.

3. Results

3.2. Changes in gully networks and volumes since 1963

Table 2 presents the results of the gully network and volume development analysis. For each catchment and period, data are given on the gully length (L, km), the length of the high-active gullies ($L_{high\text{-}active}$, km), the length of the low-active gullies ($L_{low\text{-}active}$, km) and the total gully volume (V, 10^3 m³). Given the catchment area (A, km²), the drainage density of the total gully network (D_{total}, km km^{-2}), the drainage density of the high-active gullies ($D_{high\text{-}active}$, km km^{-2}) and the area-specific gully volume (V_a, 10^3 m³ km^{-2}) could also be calculated. The development of D_{total}, $D_{high\text{-}active}$ and V_a through time is shown on Figure 3A-C and E-F.

Table 2: Gully network and volume development for the studied catchments (in total 123 km²) over the period 1963-2010.

Catchment		1963 - 1965								1986							
		L (km)	$L_{high\text{-}active}$ (km)	$L_{low\text{-}active}$ (km)	V (10^3 m³)	A (km²)	D_{total} (km km^{-2})	$D_{high\text{-}active}$ (km km^{-2})	V_a (10^3 m³ km^{-2})	L (km)	$L_{high\text{-}active}$ (km)	$L_{low\text{-}active}$ (km)	V (10^3 m³)	A (km²)	D_{total} (km km^{-2})	$D_{high\text{-}active}$ (km km^{-2})	V_a (10^3 m³ km^{-2})
	Ablo May Mekdan	96.65	62.25	34.4	2321	44.73	2.16	1.39	51.89								
	May Ba'ati	4.82	3.85	0.98	38	4,00	1.2	0.96	9.48								
	May Tsimble				0.00												
	Atsela	10.40	2.88	7.52	64	4.94	2.11	0.58	12.88	17.91	17.91	0,00	196	4.94	3.63	3.63	39.66
	Ayba	49.42	8.82	40.61	452	33.8	1.46	0.26	13.36	84.52	76.63	7.89	1217	37.00	2.28	2.07	32.9
	Seytan	8.43	(a)	(a)	90	3.91	2.16	(a)	22.95	22.12	22.12	0.00	306	8.27	2.68	2.68	37.03
	Lake Ashenge	2.52	0.74	1.78	17	1.1	2.29	0.67	15.01	2.82	2.16 [b]	0.22 [b]	24	1.1	2.56	2.23	22.25
	Total	172.23	78.53	85.27	2980	92.48	1.86	0.89	32.23	127.37	118.82	8.11	1719	51.3	2.48	2.32	33.52
	Total shale	96.65	62.25	34.4	2321	44.73	2.16	1.39	51.89								
	Total volcanics	70.76	12.43	49.9	622	39.84	1.78	0.31	15.6	127.37	118.82	8.11	1719	51.3	2.48	2.32	33.52

	1974							
May Ba'ati	6.49	5.46	1.04	60	4.00	1.62	1.36	15.06

Catchment		1994								2008- 2010							
		L (km)	$L_{high\text{-}active}$ (km)	$L_{low\text{-}active}$ (km)	V (10^3 m³)	A (km²)	D_{total} (km km^{-2})	$D_{high\text{-}active}$ (km km^{-2})	V_a (10^3 m³ km^{-2})	L (km)	$L_{high\text{-}active}$ (km)	$L_{low\text{-}active}$ (km)	V (10^3 m³)	A (km²)	D_{total} (km km^{-2})	$D_{high\text{-}active}$ (km km^{-2})	V_a (10^3 m³ km^{-2})
	Ablo	7.79	7.79	0.00	89	15.52	0.5	0.5	5.76	7.84	0.74	7.1	69	15.52	0.5	0.05	4.43
	May Mekdan	126.79	111.41	15.37	4209	44.73	2.83	2.49	94.09	100.63	87.81	12.82	3266	44.73	2.25	1.96	73.01

May Ba'ati	10.81	10.81	0.00	159	4,00	2.7	2.7	39.77	12.1	1.48	10.62	135	4,00	3.02	0.37	33.7
May Tsimble	29.4	29.4	0.00	971	8.14	3.35	3.35	119.26	30.41	29.32	1.09	1002	8.14	3.22	3.16	123.15
Atsela	17.23	17.23	0.00	186	4.94	3.49	3.49	37.59	16.66	0,00	16.66	120	4.94	3.37	0.00	24.4
Ayba	89.77	84.01	5.76	1270	37.00	2.43	2.27	34.33	75.25	57.95	17.3	1059	37.00	2.03	1.57	28.63
Seytan	27.7	27.7	0.00	422	8.27	3.35	3.35	51.11	26.16	26.04	0.12	385	8.27	3.16	3.15	46.59
Lake Ashenge									2.78	1.23	1.55	20	1.1	2.53	1.12	18.02
Total	309.47	288.34	21.14	7306	122.6	2.52	2.35	59.59	271.83	204.57	67.26	6056	123.7	2.2	1.65	48.96
Total shale	156.18	140.81	15.37	5179	52.87	2.95	2.66	97.96	131.05	117.13	13.91	4268	52.87	2.48	2.22	80.73
Total volcanics	134.7	128.94	5.76	1878	50.2	2.68	2.57	37.42	120.85	85.23	35.63	1585	51.3	2.36	1.66	30.89

L: Total gully length; $L_{high\text{-}active}$: Length of the high-active gullies; $L_{low\text{-}active}$: Length of the low-active gullies; V: Total gully volume; A: Catchment area; D_{total}: Drainage density of the total gully network; $D_{high\text{-}active}$: Drainage density of the high-active gullies, V_a: area-specific gully volume.

(a) Could not be calculated due to the poor quality of the aerial photographs. (b) 493 m of gullies were poorly visible due to shadow.

258

259

In 1963-1965, D_{total} ranged between 1.20 km km^{-1} and 2.29 km km^{-2}, and was on average 1.86 km km^{-2}. From Table 2 and Figure 3B, it can be observed that only a limited part of the 1963-1965 network was composed of high-active gullies, $D_{high\text{-}active}$ being on average 0.89 km km^{-2}. The bulk of the 1963-1965 network consisted of low-active gullies. Summed over all the study areas that could be observed in 1963-1965, the gully volume was 2,980 10³ m³. V_a varied between 9.48 10³ m³ km^{-2} and 51.89 10³ m³ km^{-2}, with an average of 32.23 10³ m³ km^{-2}. As can be observed in Table 2 and on Figure 3E-F, V_a was on average 3.3 times larger when comparing the May Mekdan catchment, that developed in shale, to the catchments that developed in volcanics. For the catchment of May Ba'ati, which could be observed on 1974 aerial photographs, the situation after a decade showed that D_{total} increased from 1.20 km km^{-2} to 1.62 km km^{-2}. This increase of 35% was the result of the expansion of the gully network with high-active gullies, and was accompanied with a strong increase in V_a, from 9.48 10³ m³ km^{-2} to 15.06 10³ m³ km^{-2}.

In 1986, a strong increase in D_{total} occurred for the catchments of Atsela, Ayba (Figure 4), Seytan and Lake Ashenge. Network expansion resulted in high D_{total} values that ranged between 2.28 km km^{-2} and 3.63 km km^{-2}, with an average of 2.48 km km^{-2}. These figures reflect closely $D_{high\text{-}active}$, as nearly all gullies could be classified as high-active. Especially for the catchment of Atsela, a strong increase in D_{total} and $D_{high\text{-}active}$ could be observed, with 72% and 523% respectively. Considering V_a, the average doubled in the study areas that developed in volcanics, increasing from 15.60 10³ m³ km^{-2} to 33.52 10³ m³ km^{-2} (range 22.25-39.66 10³ m³ km^{-2}).

In 1994, the average D_{total} and $D_{high\text{-}active}$ were at their highest value, being 2.52 km km^{-2} and 2.35 km km^{-2} respectively. D_{total} and $D_{high\text{-}active}$ both ranged between 0.50 km km^{-2} and 3.35 km km^{-2}. The low minimum D_{total} and $D_{high\text{-}active}$ values were caused by observations in the Ablo

283 catchment, which was only studied since 1994. On Figure 3B, it can clearly be observed that for
284 the period 1986-1994, the gully network was in a very active phase, with most of the gullies
285 being high-active while important network extensions took place. The total volume of the 1994
286 networks was 7,306 10^3 m³, which is more than the double of the 1963-1965 situation. V_a was on
287 average 59.59 10^3 m³ km^{-2}, and V_a-values were on average 2.6 times higher in shale catchments
288 than in volcanics catchments. The highest value for V_a was quantified in May Tsimble (= 119.26
289 10^3 m³ km^{-2}) and the lowest in the Ablo catchment (= 5.76 10^3 m³ km^{-2}). In the steep-sloped
290 catchment of Seytan, a marked increase in V_a occurred between 1986 and 1994.
291 In 2008-2010, D_{total} decreased for most catchments, with the exception of the small catchments
292 of May Tsimble and May Ba'ati. Values for D_{total} were however still relatively high, ranging
293 between 0.50 km km^{-2} and 3.37 km km^{-2}, with an average of 2.20 km km^{-2} (Table 2, Figure 3A).
294 Hence, a sharp decline could be noted for $D_{high\text{-}active}$ in most catchments. The average $D_{high\text{-}active}$
295 dropped to 1.65 km km^{-2}, and represented 75% of the total gully network. The average V_a also
296 decreased for all areas, with the exception of May Tsimble, and was 48.96 10^3 m³ km^{-2}, ranging
297 from 4.43 to 123.15 10^3 m³ km^{-2} (Table 2, Figure 3E-F). The effect of lithology still caused V_a
298 values for catchments in shale to be on average 2.6 times larger than for catchments in volcanics.
299 Summed for all the study areas, the gully volume was 6,056 10^3 m³, which is twice the volume of
300 1963-1965, and a decrease by 17% when compared to the 1994 situation.
301

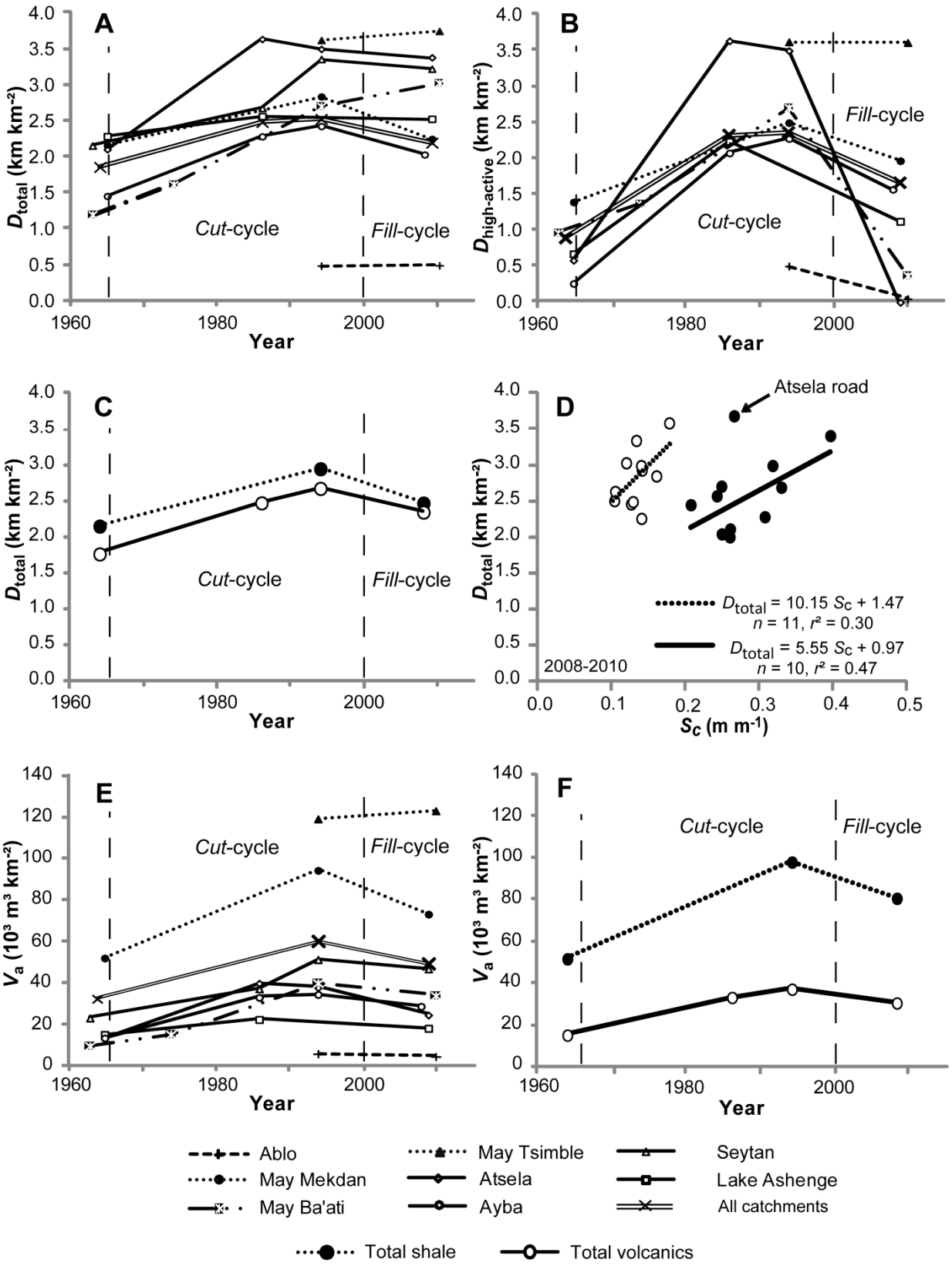
A
B
C
D
E
F
Cut-cycle
Fill-cycle
Year
D_{total} (km km^{-2})
$D_{high-active}$ (km km^{-2})
V_a (10^3 m^3 km^{-2})
Atsela road
D_{total} = 10.15 S_c + 1.47
n = 11, r^2 = 0.30
D_{total} = 5.55 S_c + 0.97
n = 10, r^2 = 0.47
2008-2010
S_c (m m^{-1})
Ablo
May Tsimble
Seytan
May Mekdan
Atsela
Lake Ashenge
May Ba'ati
Ayba
All catchments
Total shale
Total volcanics

302

303 **Figure 3**: Trends in gully drainage density and area-specific gully volume for the studied
304 catchments during the period 1963-2010. **A**: Total drainage density (D_{total}). **B**: Drainage density
305 of the high-active gullies ($D_{high\text{-}active}$), **C**: D_{total} for networks that developed in deposits derived
306 from shale and from volcanics. **D**: Relation between D_{total} and the average basin slope gradient
307 (S_c) for 2008-2010. **E**: Area-specific volume development (V_a). **F**: V_a for networks that
308 developed in deposits derived from shale and from volcanics.
309
310 A preliminary analysis on the controls on D_{total} revealed that lithology and average slope gradient
311 of the catchment (S_c, in m m^{-1}) explain a large fraction of the variability in D_{total} between
312 watersheds. As shown on Figure 3C, the overall tendency in D_{total} plots higher for shale than for
313 volcanics. The difference in D_{total} attributable to lithology was on average 0.38 km km^{-2} for the
314 period 1963-1965, 0.27 km km^{-2} in 1994 and 0.12 km km^{-2} for the period 2008-2010. In
315 percentages, these departures represent respectively 18%, 9% and 5% of increased D_{total} when
316 comparing shales to volcanics and express a slighty higher vulnerability of shales compared to
317 volcanics. Selecting 22 subcatchments <10 km^2 revealed that the distributions in D_{total} were
318 significantly different from each other when comparing catchments that developed in shale, to
319 catchments that developed in volcanics (One-way ANOVA, $P < 0.05$).
320 The effect of S_c was also added to the analysis. As shown in Figure 3D, equal values of D_{total}
321 occur on slopes with much lower S_c-values when comparing shales to volcanics. Given the
322 relative small number of observations, the linear regression lines explain relatively large
323 fractions of the variability in D_{total} (Figure 3D). Thus, slope amplifies the higher vulnerability to
324 gully erosion of soils that developed on shales when compared to soils that developed on
325 volcanics. The outlier, "Atsela road" on Figure 3D, was not considered in the linear regression.

The road zigzags in the upper catchments and clearly had an aggravating effect on gully erosion. Catchment area did not show a significant effect on D_{total} (linear regression, $n = 22$, $P = 0.09$).

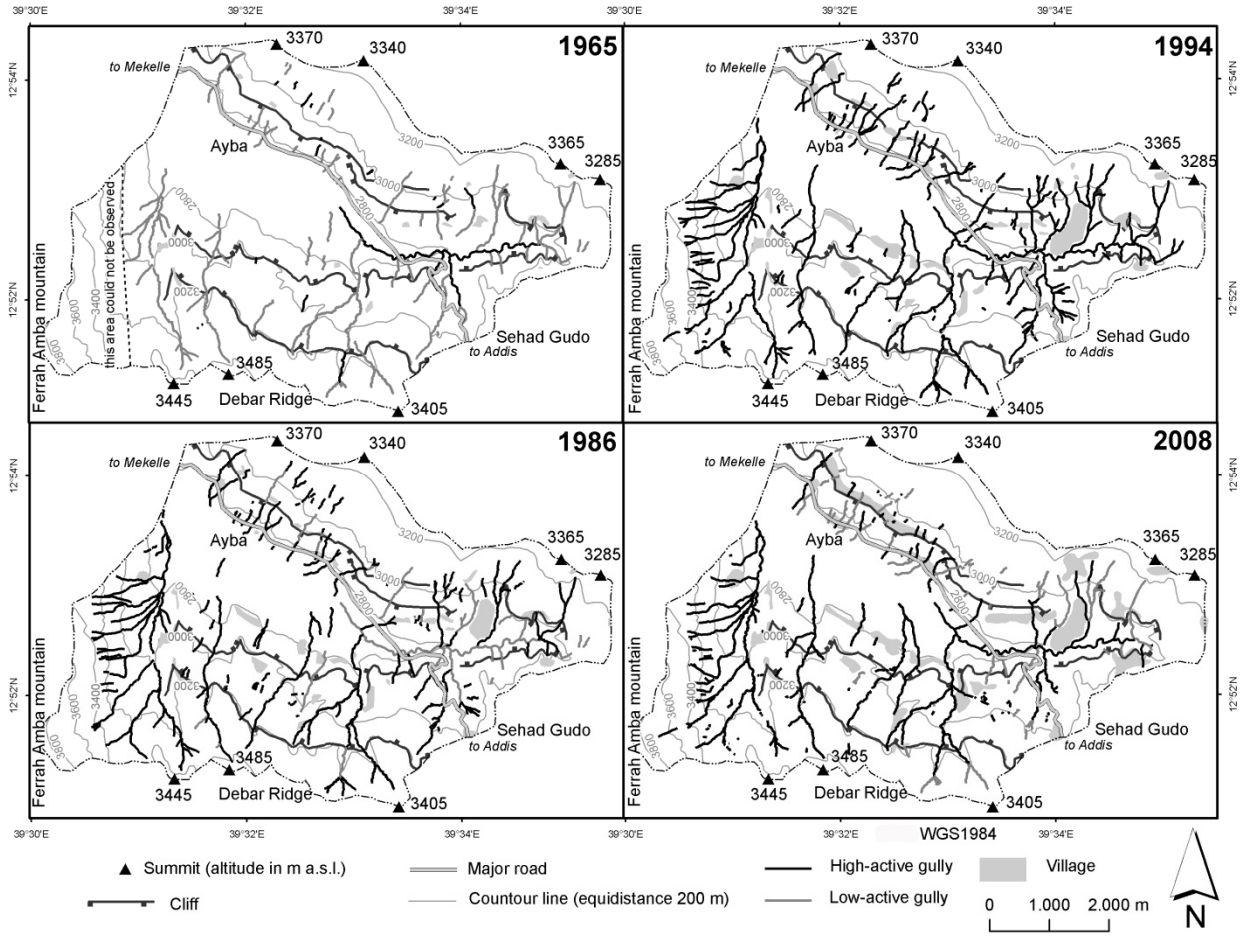

Figure 4: Gully network maps of the Ayba catchment between 1965 and 2008. Note the large proportion of low-active gullies in 1965 and the expansion (arrows for comparison) of the gully network by 1986-1994, with most gullies being high-active. By 2008, the proportion of low-active gullies increased. For details see Table 2.

4. Discussion

4.1. Using small-scale aerial photographs and Google Earth

337 Using small-scale aerial photographs proved to be very useful for the analysis of changes in
338 gully networks and volumes, even in a mountainous country like Ethiopia for which old aerial
339 photographs are of poor quality and difficult to orthorectify. This study indeed confirms that,
340 with a minimal geomorphologic background and stereographic view, gully networks can be
341 delineated with relative ease. Assessing their volumes requires the establishment of $V - L$
342 relations (Frankl et al., 2013b), based on *in situ* observations.
343 High resolution satellite images complete the recent data series for which the use of Google
344 Earth was very helpful. This platform can map features in 3D on-the-screen with a planimetric
345 accuracy comparable to that of a handheld GPS (e.g. Garmin GPSMap 60, standard deviation of
346 5 m) (Frankl et al., 2013a). With the ability to import mapped features into a GIS-environment,
347 the potential of Google Earth for geomorphologic studies is strongly increasing. Several studies
348 exist that use Google Earth, but mostly these are limited to 3D-visualizations or on-screen
349 measurements (e.g., Warren et al. 2007; Hesse, 2009; Tsou et al. 2011). Few studies explored its
350 potential for analyzing landforms (e.g., Iglesias et al., 2009; McInnes et al., 2011).
351
352 4.2. Cut-and-fill cycle
353 The changes in gully networks and volumes shown on Figure 3A-C and E-F indicate that the
354 gully system experienced a cut-and-fill cycle over the period 1963-2010. In 1963-1965, the quite
355 extensive gully network merely consisted of low-active gullies. By 1984-1994, with a marked
356 increase in high-active gullies, the gully network became highly active, with the expansion of the
357 network and the increase in gully volume as a result. At present, in 2008-2010, the proportion of
358 high-active gullies decreased at the benefit of low-active gullies. Moreover, the gully network
359 shrunk and the total gully volume decreased. This cut-and-fill cycle can best be observed when

360 considering the largest catchments, i.e. those of May Mekdan (44.7 km²) and Ayba (37 km²)
361 (Figure 3 A and E; Figure 4).
362 These findings are in line with those of Frankl et al. (2011). On the basis of repeat photography,
363 gully dynamism in Northern Ethiopia was explained in terms of hydrogeomorphic phases. From
364 ca. 1868 to 1965, gullies were low-active, displaying smooth (vegetated) cross-sections. This
365 corresponds to the large proportions of low-active gullies for the period 1963-1965 in this study.
366 It indicates that environmental vulnerability did not yet reach a critical point for large-scale
367 channel extension and degradation to occur. After 1965, a marked transition from low- to high-
368 active gullies occurred, which is also apparent in this study. This is probably related to arid
369 pulses that occurred in the 1970s and 1980s. Such phases alter biomass production and increase
370 the human pressure on land and vegetation. In order to secure food production, farmers will be
371 forced to cultivate steeper land and grazing will deplete slopes of most vegetation. Analyses of
372 region-wide land-use and cover on the basis of Landsat imagery by de Mûelenaere et al. (2012)
373 in the 1970s and 1980s confirmed that in 1984/1986, the surface covered by bare ground was
374 extensive and that the surface covered by cropland peaked. From the analysis of land-use and
375 land cover on old terrestrial photographs, Meire et al. (2012) also indicate a minimum in
376 vegetation cover in the period 1940s-1990s. Frankl et al. (2013c) showed that the length of the
377 growing period decreases with increasing drought in Northern Ethiopia, making croplands very
378 vulnerable to high-intensity rainfall in the summer rainy season. Since ca. 2000, the large-scale
379 implementation of soil and water conservation measures started to yield positive effects on the
380 environmental rehabilitation and the on stabilization of gullies. Several studies indeed indicate
381 that vegetation cover and land management strongly improved in recent decades (e.g.,
382 Gebremedhin et al., 2004; Munro et al., 2008; Alemayehu et al., 2009; Mekuria et al., 2009;

383 Nyssen et al., 2009; de Mûelenaere et al., 2012; Meire et al., 2012). Frankl et al. (2011) indicated
384 that in 2009, 23% of the studied gully sections were stabilizing. In this study, low-active gully
385 segments count for 25% of the gully network, which is very close to the previous findings.
386 The decrease in gully volume is essentially the result of siltation behind check dams on low-
387 active sections. Environmental rehabilitation proves to be very successful for gully stabilization
388 in Atsela (Figure 5). In this steep-sloped catchment, the road – built by the Italians in the 1930s –
389 that zigzags in the upper catchment causes a high runoff concentration, and strongly contributed
390 to the peaked increase in $D_{\text{high-active}}$ from 1963-1965 to 1986 (Figure 3). The sharp decline in
391 $D_{\text{high-active}}$ after 1994 is the result of a thorough land rehabilitation. The reforestation of steep
392 slopes, dense soils and water conservation structures (stone bunds, trenches) and management of
393 the gullies led to an almost total gully stabilization, where even important rainstorms, as was
394 observed multiple times in the period 2008-2011, result in little or no flooding in the gully. The
395 success of the gully rehabilitation in Atsela is most probably related to proximity to the small
396 town of Adi Shuho and the threatening by gullying of the road which used to be the main
397 thoroughfare from Addis Ababa to Mekelle. As a result, the deep gully was transformed into a
398 linear oasis (black arrow and zoom, Figure 5) which can decrease landscape fragmentation and,
399 therefore, is beneficial for ecological recovery (cf. Aerts et al., 2008). Moreover, the forestation
400 of gullies will increase their resilience to the effects of drought or land-use changes on the runoff
401 response of the land and the occurrence of flash floods in gullies. The afforestation of gullies is
402 rather rare in Northern Ethiopia and a similar example was studied for a gully near the catchment
403 of May Ba'ati (Reubens et al., 2009).
404

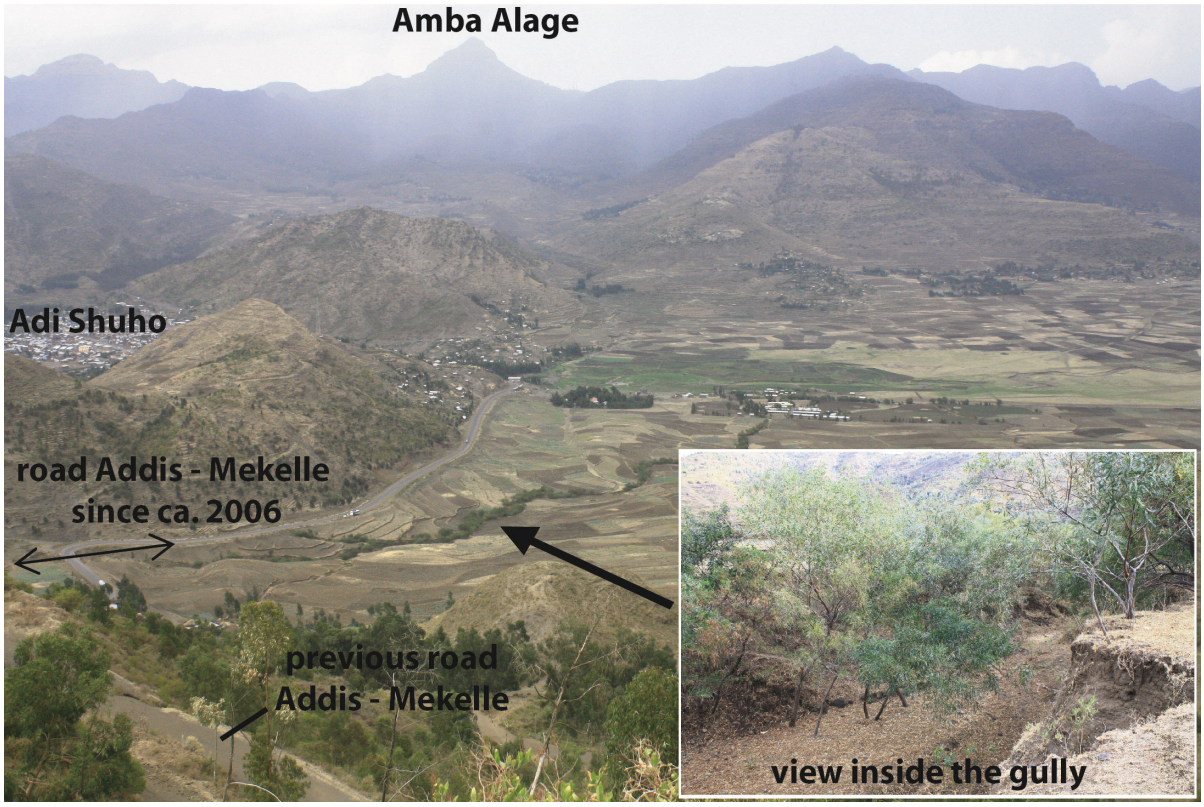

Figure 5: Gully rehabilitation in the catchment of Atsela. Thanks to the improved land management and the application of soil and water conservation measures, like the reforestation of the steep slope (foreground), the gully indicated by the black arrow was transformed into a green oasis in the landscape. (Photographs by Cleo De Wolf, March 2012)

4.3. Soil loss by gullying

In order to compare our results to other reports of soil erosion by gullying in Northern Ethiopia and in other drylands, the soil loss was also expressed as soil loss by gullying (*SL*g, t ha^{-1} y^{-1}). As no soil bulk density measurements were performed in this study, we used a standard soil bulk density of 1.5 g cm^{-3}. Average soil bulk density values for topsoils in Northern Ethiopia vary between 1.28 and 1.38 g cm^{-3} (Girmay et al., 2009).

417 Soil losses by gullying (*SLg*) are considerable in Northern Ethiopia. Over the period 1963/1965 –
418 2008/2010, the average *SLg* was 8.3 t ha^{-1} y^{-1}. This is similar soil losses of 9.7 t ha y^{-1} by sheet
419 and rill erosion (Nyssen et al., 2008b). For shales and for volcanics, the average *SLg*-values were
420 12.28 t ha^{-1} y^{-1} and 6.3 t ha^{-1} y^{-1}, respectively. Over the same period, Nyssen et al. (2006)
421 obtained average *SLg*-values of 6.2 t ha^{-1} y^{-1}, for several gullies near the catchment of May
422 Ba'ati. Low *SLg*-values of 4.1 t ha^{-1} y^{-1} were reported by Nyssen et al. (2008b) over the period
423 1998-2001 in a well managed catchment also near May Ba'ati. Calculating *SLg* over the period
424 1963/1965 - 1994, when the gully system was in a pronounced cut-phase, gave a much higher
425 value of 17.6 t ha^{-1} y^{-1}. Differentiating between shales and volcanics gave values of 27.0 t ha^{-1} y^{-1}
426 and 12.5 t ha^{-1} y^{-1} respectively. Over the period 1994-2008/2010 a net infilling of 8.3 t ha^{-1} y^{-1}
427 was calculated. This of course does not imply that no active gullying occurs (headcut retreat,
428 bank erosion, etc.), but merely indicates that soil is efficiently being trapped into gullies.
429 Compared to *SLg*-values of other dryland environments reported in Poesen et al. (2003), see
430 introduction, soil loss by gullying is severe in Northern Ethiopia.
431 These tendencies have to be understood within a socio-economic environment of strong
432 population growth and a low level of technological development, where most people rely on land
433 resources for their livelihood, and where the fragility of the country's economy is frequently
434 emphasized, for example when climatic shocks such as drought cause severe food shortages and
435 famine. Socio-economical developments and their relation to land degradation should therefore
436 be monitored closely. With an annual population growth rate of 2.37% (period 2000-2010, CSA,
437 2008) and population size which is likely to double by 2050, the country faces immense
438 challenges. The key is to rehabilitate land as a resource base for food security and ecosystem
439 services, and to strengthen and diversify the rural economy in order to make local communities

440 less dependent on land resources. Such challenges are embraced by many local, national and
441 international programs, and should remain high on the agenda.
442
443 **5. Conclusions**
444 Small-scale aerial photographs of the period 1963-1994 proved to be very valuable to map and
445 understand historical gully erosion, even for a mountainous country like Ethiopia for which old
446 aerial photographs are of poor quality and difficult to orthorectify. Having a basic geomorphic
447 background (fieldwork, use of aerial photographs) and stereographic views, gully networks could
448 be mapped relatively easily and a distinction between low- and high-active gullies could be
449 made. High-resolution satellite images offer similar resolutions to those of aerial photographs,
450 and could thus be used to collect data on present gully erosion. At no cost and at good spatial
451 accuracy, we mapped gully networks in Google Earth using 3D visualization of the images.
452 Considering the changes in gully networks and volumes from 1963 to 2010, this study confirms
453 previous findings by Frankl et al. (2011) that the gully network is experiencing a cut-and-fill
454 phase, related to alternating environmental conditions. Although network density was relatively
455 high (1.86 km km^{-2}) in the 1960s, 50% of the network was low-active, and the area specific gully
456 volume (V_a) was only 32.23 10³ m³ km^{-2}. These figures changed dramatically towards the 1980s
457 and 1990s. The total (D_{total}) and high-active ($D_{high\text{-}active}$) network density then peaked reaching
458 2.52 km km^{-2} and 2.35 km km^{-2} in 1994. This coincided with an almost double V_a of 59.59 10³
459 m³ km^{-2}. With improved land management and the region-wide implementation of soil and water
460 conservation measures in the recent decades, the gully network density and volume subsequently
461 decreased. D_{total} and $D_{high\text{-}active}$ declined to 2.2 km km^{-2} and 1.65 km km^{-2} respectively, and 25%
462 of the gully network is low-active. V_a in 2008-2010 was 48.96 10³ m³ km^{-2}. Comparing

463 catchments of similar size showed that the drainage density is largely controlled by catchment
464 gradient and that for the same gradient, densities in shales are higher than in volcanics (flood
465 basalt, rhyolites and consolidated volcanic ash).
466 Soil losses by gullying (*SL*g) are considerable in Northern Ethiopia. Over the period 1963/1965-
467 2008/2010, *SL*g was on average 8.3 t ha^{-1} y^{-1}. However, these rates have varied considerably in
468 time and space. Average *SL*g-values between shales and volcanics differ considerably. The gully
469 cut-phase from 1963/1965-1994 gave a much higher average *SL*g-values of 17.6 t ha^{-1} y^{-1}. Over
470 the period 1994-2008/2010 a net filling of 8.3 t ha^{-1} y^{-1} occurred.
471 This study shows that land degradation by gullying was indeed severe in Northern Ethiopia in
472 the second half of the 20th century. However, the huge efforts in environmental rehabilitation
473 undertaken in the recent decades are starting to result in gully stabilization. When proper land
474 management is applied, gullies can even be transformed into a linear oasis (Figure 5) which will
475 increases the resistance of gullies to possible further erosion. In the light of strong population
476 growth and expected increasing demands of land resources, rehabilitating the gully networks
477 needs to be of high priority for all local, national and international beneficiaries of soil recourses.
478

479 **Acknowledgements**
480 This study was carried out with the support of Ghent University, Research Foundation Flanders
481 (FWO), Royal Academy of Overseas Sciences, Couderé Geomatic Engineering bvba and the
482 Flemish Interuniversity Council – University Development Cooperation (VLIR-UOS-MU-Land
483 Project). Special thanks go to our field assistant Gebrekidan Mesfin and to the local residents for
484 their hospitality.
485

References

Aerts, R., Lerouge, F., November, E., Lens, L., Hermy, M., Muys, B., 2008. Land rehabilitation and the conservation of birds in a degraded Afromontane landscape in northern Ethiopia. Biodiversity and Conservation 17, 53-69.

Alemayehu, F., Taha, N., Nyssen, J., Girma, A., Zenebe, A., Behailu, M., Deckers, S., Poesen, J., 2009. The impacts of watershed management on land-use and land cover dynamics in Eastern Tigray (Ethiopia). Resources, Conservation and Recycling 53, 192-198.

Billi, P., Dramis, F., 2003. Geomorphological investigation on gully erosion in the Rift Valley and the northern highlands of Ethiopia. Catena 50, 353-368.

Boardman, J., Parsons, A.J., Holland, R., Holmes, P.J., Washington, R., 2003. Development of badlands and gullies in the Sneeuberg, Great Karoo, South Africa. Catena 50, 165-184.

Crummey, D., 1998. Deforestation in Wällo: process of illusion? Journal of Ethiopian Studies 21, 1-41.

CSA, 2008. Central Statistical Agency Federal Democratic Republic of Ethiopia population census commission. Summary and statistical report of the 2007 population and housing census. Addis Ababa.

Daba, S., Rieger, W., Strauss, P., 2003. Assessment of gully erosion in eastern Ethiopia using photogammetric techniques. Catena 50, 273-291.

de Mûelenaere, S., Frankl, A., Mitiku Haile, Poesen, J., Deckers, J., Munro, N., Veraverbeke, S., Nyssen, J., 2012. Historical landscape photographs for calibration of LANDSAT land use/cover in the Northern Ethiopian Highlands. Land Degradation and Development, online early view. DOI: 10.1002/ldr.2142

508 Descheemaeker, K., Nyssen, J., Rossi, J., Poesen, J., Mitiku Haile, Moeyersons, J., Deckers, J.,
509 2006. Sediment deposition and pedogenesis in exclosures in the Tigray Highlands,
510 Ethiopia. Geoderma 132, 291-314.
511 Frankl, A., Nyssen, J., De Dapper, M., Mitiku Haile, Billi, P., Munro, R.N., Deckers, J., Poesen,
512 J., 2011. Linking long-term gully and river channel dynamics to environmental change
513 using repeat photography (North Ethiopia). Geomorphology 129, 238-251.
514 Frankl, A., Poesen, J., De Dapper, M., Deckers, J., Mitiku Haile, Nyssen, J., 2012. Gully head
515 retreat rates in the semiarid Highlands of North Ethiopia. Geomorphology 173-174,
516 185-195.
517 Frankl, A., Zwertvaegher, A., Poesen, J., Nyssen, J., 2013a. Transferring Google Earth
518 observations to GIS-software: Example from gully erosion study. International Journal
519 of Digital Earth 6, 196-201.
520 Frankl, A., Poesen, J., Scholiers, N., Jacob, M., Mitiku Haile, Deckers, J., De Dapper, M.,
521 Nyssen, J., 2013b. Factors controlling the morphology and volume (V) – length (L)
522 relations of permanent gullies in the Northern Ethiopian Highlands. Earth Surface
523 Processes and Landforms, in press. DOI: 10.1002/esp.3405.
524 Frankl, A., Jacob, M., Mitiku Haile, Poesen, J., Deckers, J., Nyssen, J., 2013c. Spatio-temporal
525 variability of cropping systems and crop land cover with rainfall in the Northern
526 Ethiopian Highlands. Soil Use and Management, in press.
527 Gebremedhin, B., Pender, J., Tesfay, G., 2004. Collective action for grazing land management in
528 crop-livestock mixed systems in the highlands of northern Ethiopia. Agricultural
529 Systems 82, 273-290.

530 Girmay Gebresamuel, Singh, B.R., Nyssen, J., Borrosen, T., 2009. Runoff and sediment-
531 associated nutrient losses under different land-uses in Tigray, Northern Ethiopia.
532 Journal of Hydrology 376, 70-80.
533 Hesse, R., 2009. Do swarms of migrating barchan dunes record paleoenvironmental changes? -
534 A case study spanning the middle to late Holocene in the Pampa de Jaguay, southern
535 Peru. Geomorphology 104, 185-190.
536 HTS, 1976. Tigrai Rural Development Study (TRDS). Hunting Technical Services Ltd.
537 Government of Ethiopia and UK Ministry of Overseas Development, Hunting Technical
538 Services, Borehamwood.
539 Hughes, M.L., McDowell, P.F., Marcus, W.A., 2006. Accuracy assessment of georectified aerial
540 photographs: Implications for measuring lateral channel movement in a GIS.
541 Geomorphology 74, 1-16.
542 Iglesias, G., Lopez, I., Castro, A., Carballo, R., 2009. Neural network modelling of planform
543 geometry of headland-bay beaches. Geomorphology 103, 577-587.
544 James, L.A., Hodgson, M.E., Ghoshal, S., Latiolais, M.M., 2012. Geomorphic change detection
545 using historic maps and DEM differencing: The temporal dimension of geospatial
546 analysis. Geomorphology 137, 181-198.
547 Kassas, M., 1995. Desertification: a general review. Journal of Arid Environments 30, 115-128.
548 Katsurada, Y., 2007. Regional scaled mapping of gully erosion sensitivity in Western Kenya.
549 African Environment, Science and Technology 1, 049-052.
550 Knighton, D., 1998. Fluvial Forms and Processes – A New Perspective. Hodder Education,
551 London.

552 Leblanc, M.J., Favreau, G., Massuel, S., Tweed, S.O., Loireau, M., Cappelaere, B., 2008. Land
553 clearance and hydrological change in the Sahel: SW Niger. Global and Planetary
554 Change 61, 135-150.
555 Marzolff, I., Ries, J.B., 2007. Gully erosion monitoring in semi-arid landscapes. Zeitschrift für
556 Geomorphologie 51, 405-425.
557 McCann, J., 1997. The Plow and the Forest: Narratives of Deforestation in Ethiopia, 1840-1992.
558 Environmental History 2, 138-159.
559 McInnes, J., Vigiak, O., Roberts, A.M., 2011. Using Google Earth to map gully extent in the
560 West Gippsland region (Victoria, Australia), 19th International Congress on Modeling
561 and Simulation, Perth. http://mssanz.org.au/modsim2011, 1-7
562 Meire, E., Frankl, A., De Wulf, A., Mitiku Haile, Deckers, J., Nyssen, J., 2012. Mapping the
563 19th century landscape in Africa – warped terrestrial photographs of North Ethiopia.
564 Regional Environmental Change, online early view. DOI: 10.1007/s10113-012-0347-9
565 Mekuria, W., Veldkamp, E., Haile, M., Gebrehiwot, K., Muys, B., Nyssen, J., 2009.
566 Effectiveness of exclosures to control soil erosion and local community perception on
567 soil erosion in Tigray, Ethiopia. African Journal of Agricultural Research 4, 365-377.
568 Miller, S., 2004. Photogrammetric products, In: McGlone, J.C.,Mikhail, E.M., Bethel, J. (Eds.),
569 Manual of Photogammetry, Fifth Edition. ASPRS, Bethesda, MA, pp. 983–1013.
570 Moeyersons, J., 1989. La nature de l'érosion des versants au Rwanda. Annales, Kon. Mus. Mid.
571 Afr., Tervuren.
572 Moeyersons, J., 1991. Ravine formation on steep slopes: Forward versus regressive erosion.
573 Some case studies from Rwanda. Catena 18, 309-324.

574 Moges, A., Holden, N.M., 2008. Estimating the rate and consequences of gully development, a
575 case study of Umbulo catchment in southern Ethiopia. Land Degradation and
576 Development 19, 574-586.
577 Muhindo Sahani, 2011. Le contexte urbain et climatique des risques hydrologiques de la ville de
578 Butembo (Nord-Kivu/RDC). Unpubl. Phd. thesis, Université de Liège, Liège.
579 Munro, R.N., Deckers, J., Grove, A.T., Mitiku Haile, Poesen, J., Nyssen, J., 2008. Soil and
580 erosion features of the Central Plateau region of Tigrai - Learning from photo
581 monitoring with 30 years interval. Catena 75, 55-64.
582 Ndona, A., Truong, P., 2011. Community mobilization for the control of ravine erosion with
583 vetiver technology in the Congo. http://www.vetiver.org/ICV4pdfs/DC04.pdf
584 Nyssen, J., Poesen, J., J., M., Luyten, E., Veyret-Picot, M., Deckers, J., Mitiku Haile, Govers, G.,
585 2002. Impact of road building on gully erosion risk: a case study from the Northern
586 Ethiopian Highlands. Earth Surface Processes and Landforms 27, 1267-1283.
587 Nyssen, J., Poesen, J., Moeyersons, J., Deckers, J., Haile, M., Lang, A., 2004. Human impact on
588 the environment in the Ethiopian and Eritrean highlands - a state of the art. Earth
589 Science Reviews 64, 273-320.
590 Nyssen, J., Vandenreyken, H., Poesen, J., Moeyersons, J., Deckers, J., Mitiku Haile, Salles, C.,
591 Govers, G., 2005. Rainfall erosivity and variability in the Northern Ethiopian
592 Highlands. Journal of Hydrology 311, 172-187.
593 Nyssen, J., Poesen, J., Veyret-Picot, M., Moeyersons, J., Mitiku Haile, Deckers, J., Dewit, J.,
594 Naudts, J., Kassa Teka, Govers, G., 2006. Assessment of gully erosion rates through
595 interviews and measurements: a case study from Northern Ethiopia. Earth Surface
596 Processes and Landforms 31, 167-185.

597 Nyssen, J., Naudts, J., De Geyndt, K., Mitiku Haile, Poesen, J., Moeyersons, J., Deckers, J.,
598 2008a. Soils and land use in the Tigray highlands (Northern Ethiopia). Land
599 Degradation and Development 19, 257-274.
600 Nyssen, J., Poesen, J., Moeyersons, J., Mitiku Haile, Deckers, J., 2008b. Dynamics of soil
601 erosion rates and controlling factors in the Northern Ethiopian Highlands - towards a
602 sediment budget. Earth Surface Processes and Landforms 33, 695-711.
603 Nyssen, J., Mitiku Haile, Nauds, J., Munro, N., Poesen, J., Moeyersons, J., Frankl, A., Deckers,
604 J., Pankhurst, R., 2009. Desertification? Northern Ethiopia re-photographed after 140
605 years. Science of the Total Environment 407, 2749-2755.
606 Oostwoud Wijdenes, D., Poesen, J., Vandekerckhove, L. and Ghesquiere M. 2000. Spatial
607 distribution of gully head activity and sediment supply along an ephemeral channel in a
608 Mediterranean environment. Catena 39,147-167.
609 Poesen, J., Vandekerckhove, L., Nachtergaele, J., Oostwoud Wijdenes, D., Verstraeten, G., van
610 Wesemael, B., 2002. Gully erosion in dryland environments. In: Bull, L.J., Kirkby, M.J.
611 (Eds.), Dryland Rivers: Hydrology and Geomorphology of Semi-Arid Channels. Wiley,
612 Chichester.
613 Poesen, J., Nachtergaele, J., Verstraeten, G., Valentin, C., 2003. Gully erosion and
614 environmental change: importance and research needs. Catena 50, 91-133.
615 Reubens, B., Poesen, J., Nyssen, J., Leduc, Y., Amanuel Zenebe, Sarah Tewoldeberhan, Bauer,
616 H., Kindeya Gebrehiwot, Deckers, J., Muys, B., 2009. Establishment and management
617 of woody seedlings in gullies in a semi-arid environment (Tigray, Ethiopia). Plant Soil
618 324, 131-156.

619 Stocking, M.A., 1980. Examination of factors controlling gully growth. In: De Boodt, M.,
620 Gabriels, D. (Eds.), Assessment of Erosion. Wiley, Chichester.
621 Thornthwaite, C.W., 1948. An approach toward a rational classification of climate. Geogr.
622 Rev. 38, 55-94.
623 Tsou, C-Y., Feng, Z-Y., Chigira, M., 2011. Catastrophic landslide induced by Typhoon Morakot,
624 Shiaolin, Taiwan. Geomorphology 127, 166-178.
625 UN-DDD, 2012. United Nations Decade for Deserts and Fight Against Desertification
626 (UNDDD). http://unddd.unccd.int/.
627 UNEP, 1994. United Nations Convention to Combat Desertification (UNCCD).
628 http://www.unccd.int/.
629 Valentin, C., Poesen, J., Li, Y., 2005. Gully erosion: Impacts, factors and control. Catena 63,
630 132-153.
631 Virgo, K.J., Munro R.N., 1978. Soil and erosion features of the Central Plateau region of Tigrai,
632 Ethiopia. Geoderma 20, 131-157.
633 Warren, A., Chappell, A., Todd, M.C., Bristow, C., Drake, N., Engelstaedter, S., Martins, V.,
634 M'Bainayel, S., Washington, R., 2007. Dust-raising in the dustiest place on earth.
635 Geomorphology 92, 25-37
636 Williams, M., Williams, F., 1980. Evolution of the Nile basin. In, Williams, M., Faure, H. (Eds.),
637 The Sahara and the Nile. Quaternary Environments and Prehistoric Occupation in
638 Northern Africa. Balkema, Rotterdam.